PHYSICAL REVIEW E **82**, 026310 (2010)

Flow characteristics and exchange in complex biological systems as observed by pulsed-field-gradient magnetic-resonance imaging

N. M. Homan, B. Venne, and H. Van As*
Laboratory of Biophysics and Wageningen NMR Centre, Wageningen University, Dreijenlaan 3, 6703 HA Wageningen, The Netherlands
(Received 14 January 2010; published 17 August 2010)

Water flow through model porous media was studied in the presence of surface relaxation, internal magnetic field inhomogeneities and exchange with stagnant water pools with different relaxation behavior, demonstrating how the apparent flow parameters average velocity, volume flow and flow conducting area in these situations depend on the observation time. To investigate the water exchange process a two component biological model system consisting of water flowing through a biofilm reactor (column packed with methanogenic granular sludge beads) was used, before and after a heat treatment to introduce exchange. We show that correction of the stagnant fluid signal amplitude for relaxation at increasing observation time using the observed relaxation times reveals exchange between the two fractions in the system. Further it is demonstrated how this exchange can be quantified.

DOI: 10.1103/PhysRevE.82.026310 PACS number(s): 47.56.+r, 05.60.−k, 47.15.Rq

I. INTRODUCTION

Fluid transport and processes of water exchange are of great importance in many areas of science and technology, e.g., flow in (woody) plants, perfusion in human and animal tissues, transport in geological media, two-phase flow in oil recovery, hydrodynamics in chromatographic columns for molecular separation, and flow in bio-reactors and catalysis systems. Nuclear magnetic resonance (NMR) has become an important method for characterizing such porous (bio-)systems. Pulsed field gradient (PFG) NMR is a powerful tool for investigating transport processes in such systems because it allows the measurement of the displacement propagator, the probability distribution of diffusive and advective molecular displacements (for some recent reviews see [1,2]). The combination of magnetic resonance imaging (MRI) and PFG methods allows flow to be spatially resolved and flow characteristics, like velocity, volume flow and flow conducting area, can be measured per pixel, even in pixels that contain flowing and nonflowing fluid [3–5].

PFG NMR propagator measurements have been successfully applied to a direct and detailed experimental study of the topological and dynamic aspects involved in the exchange of small, nonsorbed fluid molecules between the intraparticle pore network and the interparticle void space in chromatographic columns packed with spherical shaped, porous particles [6,7]. The approach provided quantitative data of the diffusion-limited exchange kinetics for solute diffusion into and out of spherical particles. Using a systematic variation of the observation time, the time between the position encoding and decoding gradient pulses, the kinetics of mass transfer between the stagnant and flowing fluids within the packed bed could be recorded [7]. The system used in that study was in some sense ideal: no difference in relaxation between the flowing fluid in the voids and the fluid in the porous particles was observed. In addition, no surface relaxation was present in that system. Under these conditions, the signal amplitude of the stagnant fluid phase as a function of the observation time could be used directly to quantify the exchange. In many realistic (bio-)systems we have to deal with surface relaxation, internal field gradients due to susceptibility differences (e.g., between the fluid and matrix) and differences in relaxation times between pools of exchanging flowing and stagnant water.

In realistic systems internal field gradients result in attenuation of the NMR signal and shortening of the observed relaxation times. In order to measure the NMR signal accurately, suppression of the background gradients is crucial. For example, the effect of spatially constant gradients can be compensated for by a combination of bipolar gradients and refocusing pulses [8–10]. However, for long observation times (Δ) when the spin displacement becomes comparable to the length scale of local structures (pore size or particle length) the internal field gradients are not spatially constant. The measured NMR signal in a heterogeneous field for long Δ is therefore susceptible to a variation of background gradients. In addition, surface relaxation and differences in relaxation time between the exchanging flowing and stagnant fluid pools will affect the signals of the stagnant and flowing fluid. For these reasons in realistic (bio-)systems the propagator may be distorted and flow characteristics become dependent on the observation time [11]. The effect of exchange under these conditions has not yet been investigated systematically. In this respect, the use of realistic model systems may help our understanding of the transport processes of fluid in porous media.

In this paper, we focus on a range of Δ no longer than a few hundreds of milliseconds. This time range is typical for measurements where the asymptotic long-time limit for exchange cannot be reached because the relaxation times are too short. The main goal of this paper is to describe quantitatively how apparent parameters of flow (velocity, volume flow, flow conducting area) measured in a thin slice of fluid flowing in porous media depend upon the mechanisms causing the attenuation of the PFG MRI signal, including exchange. Based on this investigation we clearly show the limitation of the pulsed-field gradient stimulated echo (PGF-

*Corresponding author; Henk.vanAs@wur.nl

STE) method as well as its potential applicability for flow measurements in the porous media. We also investigate exchange between the flowing and stagnant fluid phases in a complex biological system with susceptibility and local gradient effects, surface relaxation and differences in relaxation between exchanging fluid pools and present a method to quantify this exchange.

II. THEORY

In order to apply a wide range of Δ values, PFG-STE-turbo spin echo (TSE) or -multispin echo (MSE) sequence was used, the latter being used for correlated displacement-transverse (T_2) relaxation measurements [3,12,13]. In the PFG-STE method the gradient pulses are separated by a storage interval. During the time the magnetization is in the x,y plane (the periods between the first and second and between the third 90° and first 180° pulses), the magnetization vector is sensitive to T_2 relaxation decay, the applied field gradient and the (local) background fields produced by susceptibility differences between fluid and matrix. During the storage interval (between the second and the third 90° pulses) the magnetization is stored in the direction parallel to the main magnetic field, and the magnetization is only attenuated by longitudinal (T_1) relaxation.

For the ideal PFG-STE propagator experiment the echo amplitude can be written as

$$S(q,\Delta) = S(0,\Delta)\int_R dRP(R,\Delta)e^{i2\pi qR}. \tag{1}$$

$S(0,\Delta)$ is the amplitude of the total proton magnetization in the measured volume. The displacement probability distribution (propagator) $P(R,\Delta)$ gives the probability that a molecule will travel a displacement R in time Δ in the direction of the applied magnetic field gradient pulse, that has an amplitude g and duration δ. q is defined by

$$q = \frac{1}{2\pi}\gamma\delta g. \tag{2}$$

Thus, $P(R,\Delta)$ can be reconstructed from the amplitude of the first echo as a function of g by Fourier transformation. Any molecule in a flowing fluid participates simultaneously in the coordinated mass flow and diffusional motion. The echo attenuation that occurs due to the diffusional motion, characterized by the diffusion coefficient D, over time Δ, including the T_1 and T_2 relaxation of magnetization, is written as [14]

$$S(q,\Delta) = S(0,\Delta)\exp\left[-4\pi^2q^2D\left(\Delta-\frac{\delta}{3}\right)-\frac{(\tau_2-\tau_1)}{T_1}-\frac{2\tau_1}{T_2}\right]. \tag{3}$$

τ_1 and τ_2 denote the time of the second and third 90° radio frequency (r.f.) pulses in the PFG-STE experiment. In the experiments with differing observation time Δ τ_2 was varied, but τ_1 was fixed. Thus, the contribution of T_2 in echo signal attenuation at different observation times was constant and the difference in echo amplitude at different Δ is due to T_1 relaxation only.

The flow conducting area (A) and the volume flow (Q) and the average flow velocity (v), can be calculated from the propagator [15]

$$A = \sum_{R=0}^{R_{\max}} P_c(R,\Delta)A_{\mathrm{ref}}, \tag{4}$$

$$Q = \sum_{R=0}^{R_{\max}} P_c(R,\Delta)R\frac{A_{\mathrm{ref}}}{\Delta}, \tag{5}$$

$$v = \frac{Q}{A} = \frac{\sum_{R=0}^{R_{\max}} P_c(R,\Delta)R}{\sum_{R=0}^{R_{\max}} P_c(R,\Delta)\Delta}. \tag{6}$$

Here P_c is the propagator of flowing water P_F divided by the average pixel integral I_{ref} of a propagator of the pixels in a reference tube that is filled with pure water

$$P_c(R,\Delta) = \frac{P_F(R,\Delta)}{I_{\mathrm{ref}}}. \tag{7}$$

In the real situation of flow through porous media the measured propagator can be distorted due for the following reasons [11]:

(i) First, the diffusion of molecules across the streamlines and between the stagnant and flowing fluid. Diffusion does not result in a net displacement of the ensemble of molecules, but shifts the spectral weight from the undisplaced and the most displaced parts of the displacement spectrum toward its mean. However, diffusion does not result in a change in the calculated A_{app}, Q_{app} or v_{app}.

(ii) Second, surface relaxation changes the shape of a propagator. Because of surface relaxation, the signal from spins located in small pores or next to the walls disappears. This results in an undercount of spins from the stagnant zones and the slowest flowing fluid located next to the walls and a corresponding over count of the fast flowing spins. The net result is a shift of the spectral weight of the propagator toward longer displacements which, as a consequence, leads to an increase in v_{app} and Q_{app}.

(iii) Third, susceptibility differences between fluid and matrix produces internal offset fields. The signal from moving spins can be lost from the measurement if during Δ they displace into a position with a significantly different internal magnetic field [11,16,17]. The internal offset fields affect the faster flowing spins and lead to a shift of the spectral weight toward shorter displacement and a decrease in v_{app} and Q_{app}.

The effects of the susceptibility and relaxation mechanisms is a function of observation time [18–20]. For very short Δ the displacement of fluid due to both diffusion and flow is small compared to the length scale of local structure. At such distances the magnetic field can be considered to be constant, the signal loss due to diffusion and flow motion is negligible, and the surface relaxation during short Δ is negligible. For an intermediate Δ the local magnetic field will change on the length scale of the diffusion and flow displace-

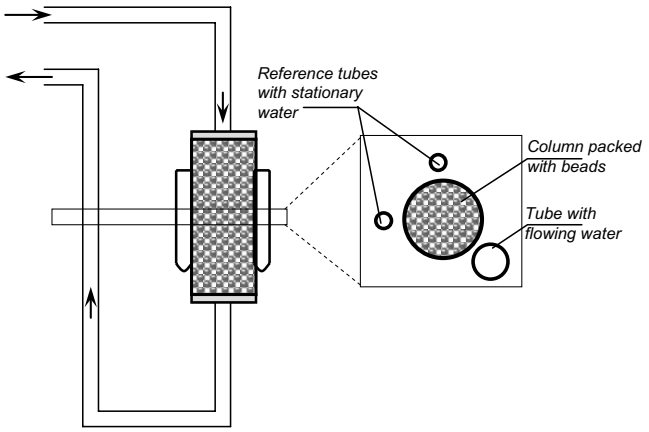

FIG. 1. Schematic representation of the phantom consisting of a column packed with porous beads, two references and a tube containing flowing water.

ment and echo loss will be observed. The elongation of Δ will also result in the progressive increase of wall relaxation effects. For a long Δ, when the diffusion shift and flow displacement are larger than the local gradient length scale, all spins in the system will then sample all possible gradient amplitudes. Under this condition the loss of magnetization will become almost constant with increasing Δ.

Susceptibility and wall relaxation effects lead to systematic uncorrected loss of magnetization, resulting in an underestimation of A_{app}. The direction of shift in v_{app} and Q_{app} from the actual values depends on which of the two mechanisms, which have opposite effects, dominates in the system at given Δ [21].

In systems with exchange between stagnant and flowing fluid (e.g., fluid inside and outside porous particles/matrix, or flowing water in vessels and stationary water in parenchyma cells for water transport in plants) the situation becomes more complicated. If differences in relaxation can be neglected, exchange between the stagnant and flowing components results in a reduction or total disappearance of the stagnant fraction and an increase of flowing fluid in the propagator as Δ increases [7,21,22]. That will result in an increase of A_{app} with increasing Δ if no susceptibility effects and differences in relaxation are present. In a system with surface relaxation the stagnant fraction disappears faster than in a system without significant surface relaxation. This effect becomes more noticeable when the measurement time scale is longer than the relaxation time of the stagnant fraction [11], and results in an additional decrease of the amplitude of the stagnant fraction. The T_1 and T_2 value for stagnant and flowing components usually varies quite significantly in different (bio-)systems. The relaxation time of fluid inside a porous matrix is in general shorter than the relaxation time of fluid outside the matrix [23], so in tree stems the stationary water in parenchyma cells has shorter T_2 than the flowing water of the xylem vessels [12,13]. Simulations of diffusion and relaxation behavior in multicompartment systems with significantly different T_2 values for the different compartments has shown that exchange between compartments results in an increase of the fraction with the longest T_2 and a decrease of the observed T_2 values [24]. From these results we expect that exchange between components with different relaxation times will cause an increase of the fraction with the longest T_2 value (the flowing fraction) and can, therefore, lead to an increase of A_{app}.

The choice of spatial resolution and slice thickness can also affect the propagator in each pixel. The dispersion in orthogonal direction (transversal dispersion) of fluid in structured media depends on the characteristic length (particles size and geometry) and the flow velocity. The mean-squared displacement perpendicular to the flow direction $\langle X^2 \rangle$ correlates to the mean displacement in the flow direction $\langle Z \rangle$ according to $\langle X^2 \rangle \propto \langle Z \rangle^{\gamma}$. From measured and simulated data it follows [25,26] that at the shortest Δ, when $\langle Z \rangle$ is considerably smaller than the particles size, the transversal dispersion displacement is about the same value as the mean displacement in the flow direction and $\gamma \approx 2$. For longer Δ and for larger flow rates the displacement in the flow direction prevails over the transversal dispersion and γ decreases. In the sequence we used, the first read out gradient was applied after first 90° pulse. Therefore, in plane dispersion during the

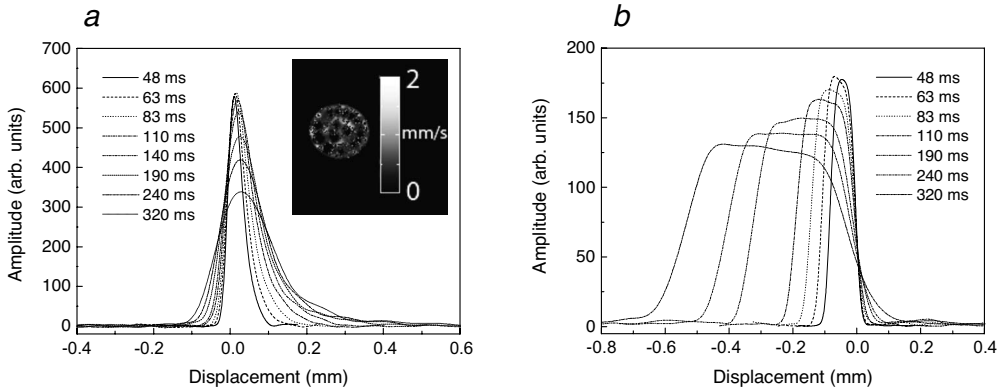

FIG. 2. The propagators in dependence of the observation time Δ for water flowing through a column packed with porous aluminum oxide beads of 3.5 mm diameter (a) and water flowing in the tube of 5 mm diameter (b). Experimental parameters: PFG-STE-TSE; resolution, 312 by 312 by 3000 μm; spectral width 50 kHz; TE1, 6.1 ms; TE, 6 ms; TR, 1000 ms; turbo factor 8; number of averages 2; 32 PFG steps; δ=1.25 ms; Δ=48, 63, 83, 110, 140, 190, 240, and 320 ms, and $\mathrm{PFG}_{\mathrm{max}}$=0.8, 0.61, 0.46, 0.35, 0.28, 0.2, 0.16, and 0.12 T/m, respectively. Inset shows the velocity-encoded image for water flow through a packing of porous beads measured at Δ=48 ms.

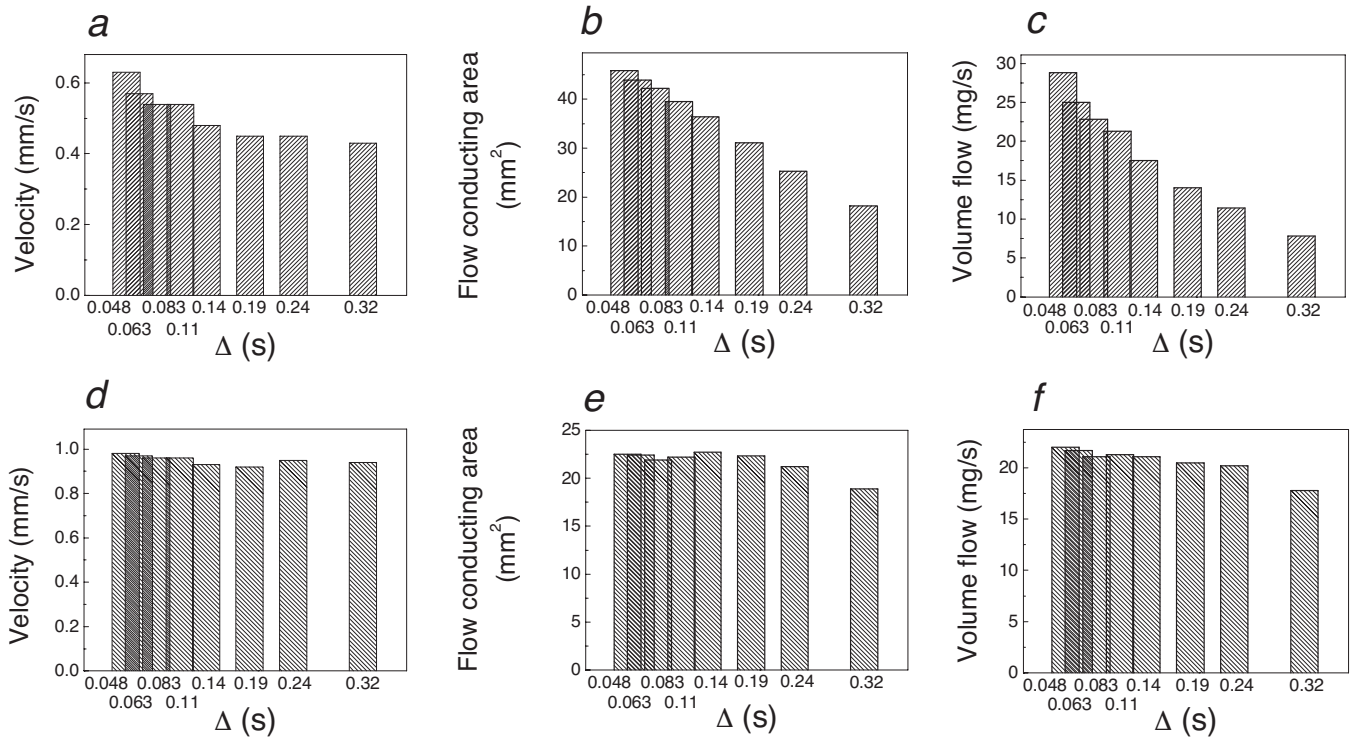

FIG. 3. Average flow velocity (a, d), flow conducting area (b, e) and volume flow (c,f) as a function of observation time Δ measured in the column packed with porous beads (a, b, c) and in the tube (d,e,f). Results extracted from the propagators presented in Fig. 2.

time between first and second read out gradients will result in attenuation of the signal and the effect will depend on Δ. This signal loss due to dispersion can be hardly compensated for by calculations. Since the local value of transversal dispersion for the given media structure and fixed Δ depends on the local velocity, the dispersion attenuation is stronger for faster flowing spins. Thus, dispersion in porous media affects the measured propagator the same way as the susceptibility mechanism.

In order to apply long Δ's in the system with short relaxation times, PFG-STE was used. To minimize the artifacts that originate from the deviation of flip angles from 90° and 180°, three slice selective 90° pulses were applied with thickness of several (3–5) millimeters. Due to flow in the direction perpendicular to the slice, part of the fluid can leave the slice during the displacement encoding time interval, which will result in an outflow effect that affects the signal intensity of fastest flowing spins. The loss of the signal from the fastest moving spins causes a shift of the spectral weight toward shorter displacements and a decrease in v_{app}, Q_{app}, and A_{app}. In contrast to loss of magnetization due to susceptibility, the magnitude of signal attenuation due to outflow is a linear function of Δ and can be compensated by correcting the propagator for the amount of fluid that has flown out of the slice.

III. EXPERIMENTAL

We performed all experiments by passing distilled water through a column comprising of randomly packed particles (see Fig. 1). Three different types of particles were used: (i) porous aluminum oxide beads of 3.5 mm diameter packed in a column with 10 mm inside diameter and 420 mm length, (ii) silicone cylinders with a diameter of about 5 mm and length of 10 mm packed in a column with an inner diameter of 14 mm and a length of 800 mm, and (iii) methanogenic granular sludge particles with diameter about 2 mm packed into a column with an inner diameter of 14 mm and a length of 800 mm. The maximum local Reynolds numbers were 7 (i), 6.5 (ii) and 6 (iii). That corresponds to the intermediate regime between creeping flow and viscous-inertial flow [27]. These systems represent three different situations. The system (i) has strong surface relaxation effects (T_2 of water inside the pores of the beads is around 1 ms) and is expected to contain local gradients due to susceptibility effects between the fluid and the solid matrix. The system (ii) presents a more ideal system without strong surface relaxation and susceptibility artifacts. The system (iii) combines the effects of wall relaxation and susceptibility, and observable stagnant water in the granules and flowing water outside the granules, with different relaxation time for the two water pools. In addition, the system can be manipulated to induce exchange between these two water pools by heating the complete packed column to 70 °C for 30 min. This treatment caused the bacterial cell membranes to become leaky allowing exchange between the intragranular and extragranular water pools.

To prevent loss of the particles due to flow and to provide an even distribution of fluid streamlines at the inlet, two cotton plugs were placed at the inlet and the outlet of the column. The column was connected to a reservoir by plastic tubes of 5 mm diameter. Tubes filled with 2% solution of agarose containing water doped with $CuSO_4$ served as refer-

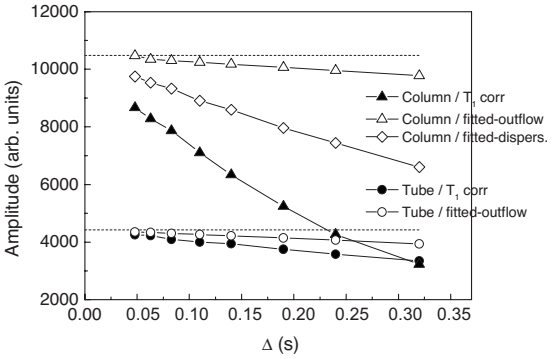

FIG. 4. Amplitude of first echo [corrected for T_1, according to Eq. (3)] in the column packed with beads (▲) and the tube with flowing water (●) as a function of observation time Δ. Actual amplitudes (extrapolated to Δ=0) in column and tube with flowing water are shown as dashed lines. Actual amplitudes corrected for out-flow effect in column (△) and tube with flowing water (○). Actual amplitude corrected for dispersion attenuation by the read out gradients in the column packed with beads (◇). The experimental parameters are the same as mentioned in Fig. 2.

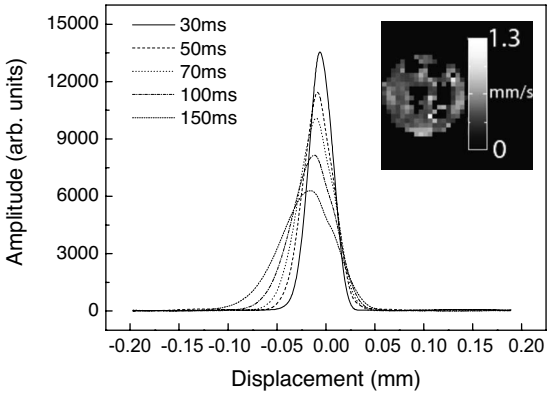

FIG. 5. The propagator at different Δ for water flow in a column packed with silicon cylinders (diameter around 5 mm and length 10 mm). Experimental parameters: PFG-STE-MSE; resolution, 844 by 844 by 5000 μm; spectral width 50 kHz; TE1, 13.5 ms; TE, 4.8 ms; TR, 2000 ms; number of averages 2, 2, 2, 4, and 4; 48 PFG steps; Δ=30, 50, 70, 100, and 150 ms; δ=4 ms; $\mathrm{PFG}_{\max}$ =0.36 T/m. Inset shows the velocity-encoded image for water flow through a packing of silicon cylinders measured at Δ=30 ms.

ences. The volume flow during a single set of measurements was constant.

A 3 T MRI system was used based on a superconducting magnet with a 50 cm vertical free bore (Magnex, Oxford, U.K.), in combination with an Avance console (Bruker, Karlsruhe, Germany) [12]. An openable gradient coil was used with a maximum gradient strength of 1 T/m. For T_2 relaxation time measurements a MSE sequence was applied (see details in [5]); a 32×32 matrix was used, the field of view was 28.5×28.5 mm^2, and the slice thickness was 5 mm. Measurements were performed with an echo time (TE) of 4.8 ms and a repetition time (TR) of 6 s, and 256 echoes were acquired per echo train. For each image two acquisitions were averaged to improve the signal to noise ratio. For T_1 relaxation measurements a inversion recovery (IR)-TSE sequence was used, with TE=3.6 ms.

The propagators for all our measurements were obtained by PFG-STE-TSE sequences [5]. The PFG-STE-MSE was used for correlated displacement-T_2 measurements [13]. For the flow measurements in the column packed with porous aluminum oxide beads, the maximum g was achieved in 32 equidistant steps, δ was 1.25 ms. Measurements were performed with slice thickness of 3 mm, TR=1 s, turbo factor 8. For all other flow measurements g was achieved in 48 equidistant steps, δ=4 ms, slice thickness 5 mm, TR=2 s, and turbo factor 8. In correlated flow-T_2 measurements 64 echoes were acquired per echo train, with TE=8 ms.

IV. RESULTS AND DISCUSSION

The propagators for flow in the column packed with porous beads with strong relaxation sinks and in the tube [system (i)] for different values of Δ are shown in Fig. 2. These propagators of the column and tube flow were extracted from the images by summing the propagators observed in all pixels in the column or tube, respectively. Since the signal from water inside the beads is not detectable due to having too short a T_2 (around 1 ms), the entire NMR signal in the column represents flowing fluid. The nonsymmetrical shape of the propagators in Fig. 2(a) is typical for dispersive flow. The shape of the propagator is typical for mean displacement small enough in comparison to the bead diameter, so the local displacement is proportional to the local velocity [22,28–30]. The propagators of the water flux in the tube [Fig. 2(b)] have an approximately rectangular shape typical for laminar flow smoothed by diffusional motion. Some deviation from rectangular shape for the propagator measured at the longest Δ may originate from the bend of the tube (see Fig. 1).

The values of v_{app}, A_{app}, and Q_{app} extracted from the propagators shown in Fig. 2 decrease monotonically with increasing Δ [Figs. 3(a)–3(c)]. The time dependence of these parameters is typical for dispersion, susceptibility and surface relaxation effects in the column. We do not expect susceptibility effects in the tube with water and v_{app} is nearly the same for all Δ [Fig. 3(d)]. A_{app} [Fig. 3(e)] and Q_{app} [Fig. 3(f)] slightly decreases at the longest Δ.

The summed signal amplitude of the first echo of all pixels in the column and in the tube corrected for T_1 [cf. Eq. (3)] as a function of Δ are shown in Fig. 4 (solid symbols). The total signal in the reference tubes after correction for T_1 relaxation does not depend on Δ (data not shown). The total signal amplitude in the tube measured at the longest Δ (320 ms) is slightly lower than the signal amplitude at the shortest observation time of 48 ms. The signal amplitude in the column shows a significant decrease with increasing Δ. To estimate the actual magnetization in the tube and the column, the two T_1 corrected curves were monoexponentially extrapolated to zero observation time (Fig. 4, dashed lines). The amplitudes $S(0)$ obtained by extrapolation for both fractions were corrected for outflow effect (Fig. 4, open symbols). For this correction we used the measured v_{app} of 1 mm/s in the tube [see Fig. 3(d)] and 0.63 mm/s in the column [Fig. 3(a)] and the slice thickness of 3 mm.

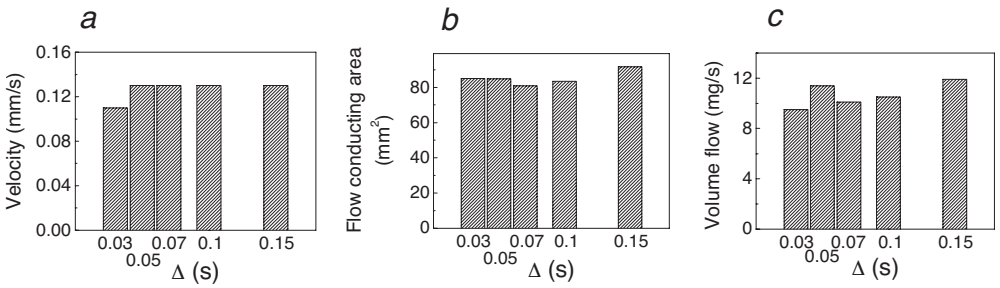

FIG. 6. Average flow velocity (a), flow conducting area (b) and volume flow (c) as a function of observation time Δ in a column packed with silicon cylinders. Results extracted from the propagators presented in Fig. 5.

The difference between the outflow corrected $S(0)$ and the T_1 corrected amplitude arises from uncorrected signal loss. Since the silicon tube surface is not a strong relaxation sink, we do not expect a significant surface relaxation, and as the magnetic field is homogenous in the tube filled with water we do not expect any signal loss due to flow in offset fields. Though diffusion of molecules across streamlines does not shift the spectral weight of propagator, it can contribute to signal loss due to the read out gradient pulses. We assumed that diffusion coefficient of fluid in the tube is equal to diffusion coefficient of bulk water 2.35×10^{-9} m^2/s [31]. Since the first read out gradient was applied after first 90° pulse in the sequence we used, the in-plane diffusion over the longest Δ (320 ms) is 39 μm (in-plane resolution is 312×312 μm^2) and this will result in uncompensated signal loss. That results in progressive decrease of Q_{app} and A_{app} with increasing Δ even when there are no significant wall relaxation and local gradients. In addition, there will be same saturation effect due to the short TR with respect to T_1. The outflow effect results in an underestimation of signal from the fastest flowing spins, slightly shifting the spectral weight of the propagator toward lower v_{app}. The total signal loss due to both outflow and diffusion leads to a greater decrease of A_{app} and Q_{app} with increasing Δ in the tube with water. These effects are much stronger in the column. Strong uncompensated signal attenuation explains the decrease of A_{app} with increasing Δ and results from the susceptibility, wall relaxation and diffusion/dispersion mechanisms. The calculated signal attenuation due to dispersion motion between first and second read out gradient pulses is shown in Fig. 4 (diamond symbols). Average dispersion displacement was estimated on the basis of displacement in the flow direction for average flow velocity 0.63 mm/s. The values of dispersion displacement were taken from literature [32]. The decrease in v_{app} with increasing Δ indicates that the outflow, dispersion and susceptibility effects are stronger than the surface relaxation effect. It has also been shown in a system without outflow effects that for long Δ the loss of slow spins exceeds the suppression of signal of fast flowing spins [21] and this results in an increase of apparent displacement at increasing Δ. For measurements with slice selective r.f. pulses, the outflow effect progressively removes the signal of the fastest flowing spins, shifting the spectral weight of the propagator toward smaller values.

To confirm that the observed systematic changes of the flow parameters arise from the susceptibility in the system, we investigated flow in a column filled with nonporous silicone cylinders [system (ii)]. The latter have smooth walls, and in comparison to the porous beads this system has lower background gradients and hardly any surface relaxation. One can then expect that the magnetization loss due to susceptibility is significantly smaller. Since the silicone cylinders have relatively big size (5 mm diameter and 10 mm length) we do not expect significant attenuation of signal due to dispersion. To minimize the outflow effect a lower velocity was used and the slice thickness was increased to 5 mm. The propagators of water flow through the column packed with these cylinders are shown in Fig. 5 for Δ ranging from 30 ms to 150 ms. They have a broad asymmetric shape indicating the predominance of slow flowing water similar to the flow through the column packed with porous beads. In Fig. 6 v_{app}, A_{app}, and Q_{app} are presented for different Δ. The values of all these parameters do not change systematically with increasing Δ. The total signal corrected for T_1 is nearly independent of Δ in both the column and in the tube (Fig. 7). Since T_1 was the same (2 s) in the tube and in the column, the partial saturation effect arising due to the relatively short TR (2 s) was the same in both parts of the system. No outflow effect was observed (Fig. 7). Because the signal amplitude in the column does not depend on Δ we can conclude that there are no susceptibility and dispersion effects. As a consequence, v_{app}, A_{app}, and Q_{app} are also independent of Δ.

In porous systems wall relaxation, dispersion and flow motion in internal magnetic field gradients result in signifi-

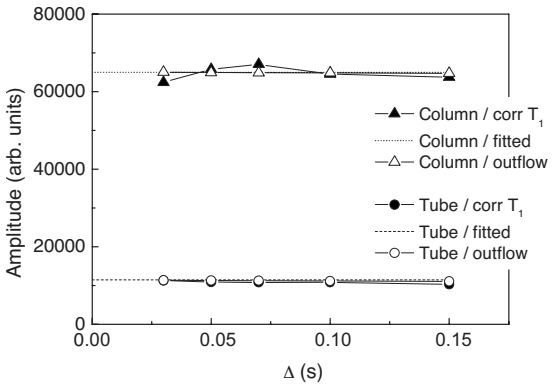

FIG. 7. The T_1 corrected first echo amplitude measured at observation time 30, 50, 70, 100 and 150 ms in the column packed with cylindrical particles (▲), tube (●). The dashed lines show the amplitude of the first echo obtained by fitting of the first echo amplitudes to zero observation time. Fitted amplitudes corrected for out-flow effect in column (△) and tube with flowing water (○). The experimental parameters are the same as mentioned in Fig. 5.

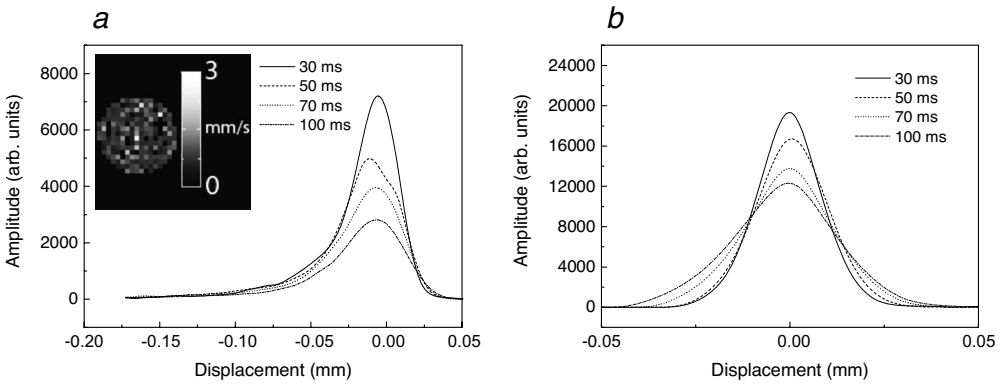

FIG. 8. T_2 resolved propagators in dependence of Δ for the extra-granular (T_2=695 ms) (a) and intragranular (T_2=12 ms) (b) components in a column packed with intact methanogenic biofilm granules. Experimental parameters: PFG-STE-MSE; resolution 891 by 891 by 5000 μm; spectral width 50 kHz; TE1, 13.5 ms; TE, 8 ms; TR, 2000 ms; 48 PFG steps; Δ=30, 50, 70, and 100 ms, and number of averages 2, 2, 2, and 4, respectively; δ=4 ms; PFG_{max}=0.41 T/m. Inset shows the velocity-encoded image for water flow through a packing of biofilm granules measured at Δ=30 ms.

cant uncorrected signal loss. To minimize the effect of susceptibility the background gradient suppression sequences were used [8,10]. However, there is no way to compensate these effects completely. The investigation of flow in porous media shows that susceptibility and wall relaxation result in systematic uncompensated signal loss and, as a consequence, to underestimation of A_{app}, Q_{app} and to shift v_{app} from its real value. Since signal loss time dependent, the deviation of apparent flow parameters from real ones increases with increasing Δ.

To investigate the effect of exchange in a multicomponent system one can measure the change in relative water content (population) of the different fractions with increasing observation time [7]. This method requires very accurate determination of the signal amplitudes of the fractions present in the system. As demonstrated above, susceptibility and surface relaxation effects affect the observed signal amplitude of flowing water and exchange processes further complicates the measurements. To investigate this problem we performed the following measurements. Tap water was flushed through a glass column with inner diameter of 17 mm and packed with a methanogenic granular sludge, originating from an anaerobic waste water bioreactor. These biofilm granules consist of rigid, well-settling microbial (spherical) aggregates (diameter around 2 mm) that develop by the mutual attachment of bacterial cells in the absence of a carrier material. Since the relaxation times for the water flowing through the column and the water in the granules are different, flowing and stagnant water fractions can be discriminated on the bases of their T_2. Correlated displacement-T_2 measurements [13] were performed to obtain the propagators for both water fractions.

To avoid outflow effects a slice thickness of 5 mm, a low velocity and relatively short Δ were used. As a result all the flow parameters for flowing water in the tube, i.e., v_{app}, A_{app}, and Q_{app}, were nearly independent on Δ (data not shown). T_2 measurements by MSE imaging of water in the column revealed two components with T_2 of 12 and 695 ms, respectively, corresponding to water in the granules and extragranular water and in agreement with previous measurements [23]. T_1 was found to be 40 and 1074 ms, corresponding to the intragranular and extragranular water, respectively. Figure 8 shows the T_2 resolved propagators of each of these two fractions with increasing Δ. The propagators related to the shortest T_2 [Fig. 8(b)] are symmetrical and centered at zero, which is typical for nonflowing water. The propagators related to the longest T_2 [Fig. 8(a)] are not symmetrical around zero displacement, indicating fluid flow. The broad peak distributed at short displacements is related to slow moving fluid around periphery granules. The v_{app}, A_{app}, and Q_{app} for Δ increasing from 30 to 100 ms are shown in Fig. 9; all three parameters decrease with increasing Δ. As demonstrated above, parameter behavior of this kind indicates strong susceptibility effects in the sample.

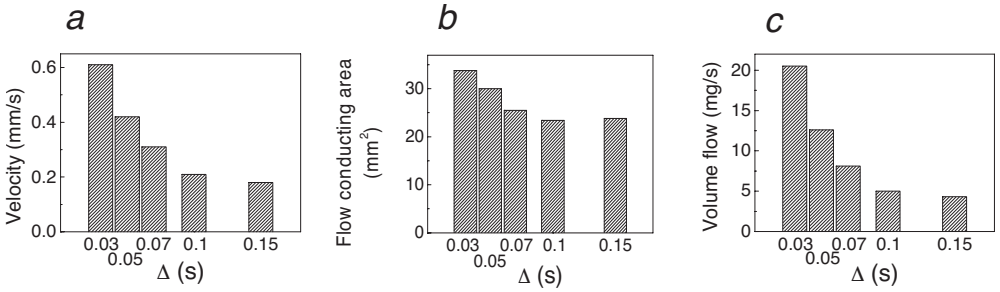

FIG. 9. Apparent average flow velocity (a), flow conducting area (b) and volume flow (c) for different observation time Δ measured for the water flow through the column packed with nontreated granules. Results extracted from the propagators presented in Fig. 8(a).

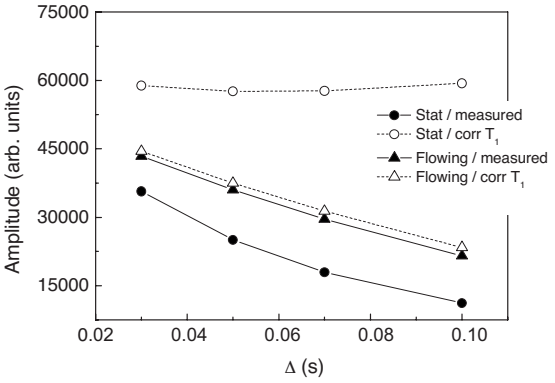

FIG. 10. T_1 corrected first echo amplitudes of intragranular water and extragranular water at observation time 30, 50, 70, and 100 ms measured in a column packed with non treated methanogenic biofilm granules. The experimental parameters are the same like mentioned in Fig. 8.

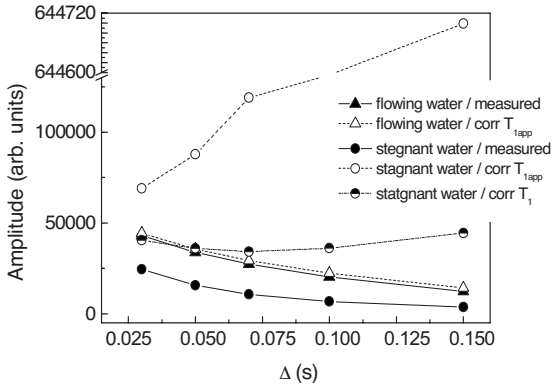

FIG. 11. Measured and T_1 corrected first echo amplitudes of intragranular and extra-granular water for observation time 30, 50, 70, 100, and 150 ms, measured in the heat treated granular bed. Experimental parameters: PFG-STE-MSE; resolution, 875 by 875 by 5000 μm; spectral width 50 kHz; TE1, 13.5 ms; TE, 4.8 ms; TR, 2000 ms; 48 PFG steps; Δ=30, 50, 70, 100, 150 ms, and number of averages 2, 2, 2, 4, and 4, respectively; δ=4 ms; PFG_{max}=0.36 T/m.

In a two-component system with no significant relaxation or susceptibility and no exchange between the stagnant and flowing water pools, the signal amplitude of both fractions corrected for relaxation will not depend on Δ. Exchange between the pools will result in a decrease of the relaxation times of both components [13,33], and an increase of the amplitude of the flowing fluid, coupled with a corresponding decrease in the amplitude of the stagnant water, with increasing Δ [7,22]. Since the signal from flowing fluid is sensitive to susceptibility effects, the amplitude of this component corrected for T_1 attenuation decreases with increasing Δ (see Fig. 10). Thus, the signal amplitude of flowing water cannot be used for the determination of exchange. At the same time the fluid inside the bacterial cells is hardly sensitive to the susceptibility effects because the displacement of spins due to diffusion inside the granules is much smaller than that due to dispersive flow outside the granules. Therefore, signal attenuation caused by the diffusive motion in magnetic field gradients inside the granules is lower than the attenuation for water flowing though the column. In Fig. 10, the first echo amplitude of stagnant granular water and of flowing water, both measured and T_1 corrected, are presented. Clearly, the T_1 corrected amplitude of the stagnant water in the granules is independent of Δ. This is typical for a system without exchange between the components.

The temperature treatment of the system resulted in a decrease of the apparent values for T_1 (29 and 988 ms) and T_2 (10 and 605 ms), revealing enhanced water exchange between the different water pools. The propagators of stagnant and flowing fluids for increasing Δ are similar to the propagators of the non-treated system (data not shown). The v_{app}, A_{app}, and Q_{app} monotonically decrease with increasing Δ (data not shown), similar to those observed in the system before the heat treatment. The first echo amplitudes of the stagnant and flowing fractions as a function of Δ are shown in Fig. 11. The values of T_1 measured for the temperature treated system were used to correct the signal attenuation with increasing Δ. After this T_1 correction, an uncorrected amplitude loss is still observed for the flowing fraction due to susceptibility effects and wall relaxation. Surprisingly, the T_1 corrected amplitude of the first echo of the stagnant intragranular water (strongly) increases with increasing Δ, and this increase is significantly higher than the loss of amplitude for the flowing fraction. The total amplitude of these two fractions after T_1 correction increases with increasing Δ, which is physically impossible. If we correct the amplitude of the stagnant fraction using the T_1 of the granular water measured for the untreated system the amplitude becomes independent on Δ, as expected for a system without exchange. Clearly, the observed T_1 is shortened by the exchange process and using this T_1 value to correct the amplitude of the stagnant water pool results in an overcorrection. If the observation times used in the measurements are of the same order as the T_1 of the stagnant fraction even a small decrease of T_1 due to exchange in the system will have a significant effect on the overcorrection of the amplitude of the nonflowing fluid. The temperature treatment clearly resulted in leakage of both the cell walls and the internal membranes of the bacterial cells, resulting in exchange of water inside the cells/granules with the flowing water pool and a decrease in the apparent T_1 of the stagnant water.

From this observation and our explanation a method can be devised to quantify the exchange. Exchange of water from the stagnant pool to the flowing pool will shorten the residence time in the stagnant pool. The observed T_1 is then given by $1/T_{1app}=1/T_{1real}+1/\tau$. Here, τ is the mean residence time of a water molecule in the stagnant water fraction. T_{1real} is the T_1 value without exchange, which results in a corrected first echo amplitude of the stagnant water pool that is independent of Δ. τ can either be diffusion limited or defined by exchange over barriers, membranes, or similar. In the heat-treated column we find with T_{1app} =29 ms, T_{1real}=40 ms a mean residence time τ=125 ms.

V. CONCLUSIONS

We have shown that in porous media the outflow, the surface relaxation and susceptibility effects induced by the

internal magnetic field gradients can (strongly) affect flow characteristics as measured by PFG-STE by removing the fastest and slowest moving spins from the NMR signal. Only the outflow effect can be corrected for by calculation. As a result, the apparent average velocity, v_{app}, the flow conducting area, A_{app}, and the volume flow, Q_{app}, as derived from the propagators, differ from their real values and become dependent on Δ. The noncorrected signal loss that remains after T_1 correction of the first echo amplitude always results in a systematic underestimation of A_{app}. Outflow and flow in local magnetic field gradients progressively remove the fastest flowing spins. When the total effect of these two mechanisms exceeds the magnetization loss from the slowest spins due to wall relaxation, the spectral weight of the propagator shifts toward lower values. That results in a reduction of v_{app}. Investigation of the dependence of the apparent flow parameters on Δ is essential for the selection of optimal parameters for flow measurement in porous biological media.

The sensitivity of the signal amplitude of the flowing fluid in inhomogeneous media to susceptibility and wall relaxation makes it impossible to use it for the determination of exchange in the system. Since the signal amplitude of the stagnant water is hardly affected by uncompensated loss it can be used to reveal exchange between the stagnant and flowing water pools. If the T_1 corrected amplitude of the stagnant fraction is independent (or decreases) of Δ no exchange is present on that time scale. Exchange between fluids with different T_1 is accompanied by a decrease in the apparent T_1 values for both fractions. In these circumstances, the correction of the amplitude of stagnant water using the apparent T_1 will result in an increase of the signal amplitude of this fraction with increasing Δ. This overcorrection of the amplitude of stagnant fluid is a clear indication of exchange between the fractions. In a system with exchange it is necessary to use the value of T_1 for the system in the absence of any exchange to correct the signal amplitude of the stagnant water so that it becomes independent of Δ. From the difference between the observed T_1 and the T_1 without exchange the mean residence time of water in the stagnant pool can be obtained.

[1] M. D. Mantle and A. J. Sederman, Prog. Nucl. Magn. Reson. Spectrosc. **43**, 3 (2003).

[2] S. Stapf and S. Han, *NMR Imaging in Chemical Engineering* (Wiley-VCH, Weinheim, 2005), Chap. 1.

[3] T. W. J. Scheenen, D. van Dusschoten, P. A. de Jager, and H. Van As, J. Magn. Reson. **142**, 207 (2000).

[4] H. Van As, J. Exp. Bot. **58**, 743 (2007).

[5] C. W. Windt, F. J. Vergeldt, P. A. de Jager, and H. Van As, Plant, Cell Environ. **29**, 1715 (2006).

[6] U. Tallarek, D. van Dusschoten, H. Van As, E. Bayer, and G. Guiochon, J. Phys. Chem. B **102**, 3486 (1998).

[7] U. Tallarek, F. J. Vergeldt, and H. Van As, J. Phys. Chem. B **103**, 7654 (1999).

[8] G. Zheng and W. S. Price, J. Magn. Reson. **195**, 40 (2008).

[9] R. M. Cotts, M. J. R. Hoch, T. Sun, and J. T. Markert, J. Magn. Reson. **83**, 252 (1989).

[10] D. van Dusschoten, P. A. de Jager, and H. Van As, J. Magn. Reson., Ser. A **112**, 237 (1995).

[11] U. M. Scheven, J. G. Seland, and D. G. Cory, Phys. Rev. E **69**, 021201 (2004).

[12] N. M. Homan, C. W. Windt, F. J. Vergeldt, E. Gerkema, and H. Van As, Appl. Magn. Reson. **32**, 157 (2007).

[13] C. W. Windt, F. J. Vergeldt, and H. Van As, J. Magn. Reson. **185**, 230 (2007).

[14] P. T. Callaghan, *Principles of Nuclear Magnetic Resonance Microscopy* (Clarendom Press, Oxford, 1993), Chap. 6.3.

[15] T. W. J. Scheenen, D. van Dusschoten, P. A. de Jager, and H. Van As, J. Exp. Bot. **51**, 1751 (2000).

[16] Y. Q. Song, Phys. Rev. Lett. **85**, 3878 (2000).

[17] P. M. Singer, G. Leu, E. J. Fordham, and P. N. Sen, J. Magn. Reson. **183**, 167 (2006).

[18] H. C. W. Donker, H. Van As, H. T. Edzes, and A. H. W. Jans, Magn. Reson. Imaging **14**, 1205 (1996).

[19] L. Lebon and J. Leblon, J. Magn. Reson. **159**, 13 (2002).

[20] N. Nestle, A. Qadan, P. Galvosas, W. Süss, and J. Kärger, Magn. Reson. Imaging **20**, 567 (2002).

[21] U. M. Scheven, J. G. Seland, and D. G. Cory, Magn. Reson. Imaging **23**, 363 (2005).

[22] D. Kandhai, D. Hlushkou, A. G. Hoekstra, P. M. A. Sloot, H. Van As, and U. Tallarek, Phys. Rev. Lett. **88**, 234501 (2002).

[23] P. Lens, F. Vergeldt, G. Lettinga, and H. Van As, Water Sci. Technol. **39**, 187 (1999).

[24] L. van der Weerd, S. M. Melnikov, F. J. Vergeldt, E. G. Novokov, and H. Van As, J. Magn. Reson. **156**, 213 (2002).

[25] S. Stapf, K. J. Packer, R. G. Graham, J.-F. Thovert, and P. M. Adler, Phys. Rev. E **58**, 6206 (1998).

[26] S. Stapf, Chem. Phys. **284**, 369 (2002).

[27] D. Hlushkou and U. Tallarek, J. Chromatogr. A **1126**, 70 (2006).

[28] L. Lebon, L. Oger, J. Leblond, J. P. Hulin, N. S. Martys, and L. M. Schwartz, Phys. Fluids **8**, 293 (1996).

[29] L. Lebon, J. Leblond, and J. P. Hulin, Phys. Fluids **9**, 481 (1997).

[30] R. Duplay and P. N. Sen, Phys. Rev. E **70**, 066309 (2004).

[31] T. L. James and G. G. McDonald, J. Magn. Reson. **11**, 58 (1973).

[32] H. Van As, W. Palstra, U. Tallarek, and D. van Dusschoten, Magn. Reson. Imaging **16**, 569 (1998).

[33] L. van der Weerd, M. M. A. E. Claessens, C. Efde, and H. Van As, Plant, Cell Environ. **25**, 1539 (2002).